

THERMO-HYDRO-MECHANICAL MODELLING OF LOW PERMEABILITY MEDIA USING A DOUBLE-POROSITY FORMULATION

M. Sánchez^{*†}, A. Gens^{*} & S. Olivella^{*}

^{*}Geotechnical Engineering Department,
Technical University of Catalonia (UPC),
Jordi Girona 1-3, Edificio D-2. 08034 Barcelona, Spain
e-mail: marcelo.sanchez@upc.es

[†]Instituto de Materiales y Suelos,
Universidad Nacional de San Juan (UNSJ).
Urquiza 35 (N). 5400 San Juan, Argentina

Key words: coupled problems, unsaturated soils, material fabric, elasto-plastic model, unsaturated non-isothermal flow, radioactive waste isolation.

Abstract. *The study of engineering problems in porous media is generally dealt with by assuming that they possess a continuous distribution of one type of voids. However, there are some media in which, for a proper handling of the problem, it is crucial to consider the different structural levels involved in the material fabric. This work presents a mathematical formulation that considers the mechanical, hydraulic and thermal problems in a fully coupled way. The Thermo-Hydro-Mechanical (THM) approach has been developed to handle engineering problems in porous media with two dominant structures of voids. The formulation allows the consideration of non-isothermal multiphase flows in both media, coupled with the mechanical and the thermal problems. The double porosity approach has been implemented in a finite element code and it has been used to analyze a variety of engineering problems. Special attention has been placed on the analysis and design of high level radioactive waste disposals. A THM modelling of a large scale heating test is also presented in this paper.*

1 INTRODUCTION

The use of expansive clays as a buffer in the design of high level radioactive waste disposals is perhaps the main motivation of many investigations tending to explore its *THM* behaviour. In the last few years, more specific tests have been performed leading to a better understanding of swelling clays behaviour. Particularly helpful have been the work in which information related to the clay fabric has been provided, revealing a strong influence of the pore structure on the *THM* behaviour of expansive materials^{[1],[2]}.

Focusing on the problem of radioactive waste repository, most conceptual designs envisage placing the canisters, containing the nuclear waste, in horizontal drifts or vertical boreholes in deep geological media. The empty space surrounding the canisters is filled by an engineered barrier often made up of compacted swelling clay (Figure 1). In this multi-barrier disposal concept both, the geological barrier (host rock) and the engineering barrier (backfill) should be media with very low permeability in order to achieve the required degree of waste isolation. Other functions that the barriers would accomplish are: to provide mechanical stability for the waste canister (by absorbing stresses and deformations) and to seal discontinuities in the emplacement boreholes and drifts, among others.

Significant *THM* phenomena take place in the engineered barrier and in the near field due to the combined actions of heating and hydration. For instance, hydration takes place from the external boundary inwards driven by the gradient between the applied water pressure and the suction in the bentonite (which is initially unsaturated). Hydration will cause a progressive rise in degree of saturation. This affects both the temperature field, due to the modifications of thermal conductivity, and the stress/strain distribution, due to suction changes. On the other hand, in the inner part of the buffer, applied heat causes a temperature rise that moves outwards. Water evaporation causes drying of the bentonite. Vapour coming from the inner part of the barrier will diffuse towards the outer regions where it will condense causing a local rise of degree of saturation. Water transfer is also affected by the dependence of water viscosity on temperature and by porosity changes arising from variations of stresses and suction^[5]. There are more significant *THM* couplings in this kind of problem^{[5],[6]}.

Therefore, according with the expressed above, coupled *THM* analyses are generally required to achieve a good understanding of this problem. Numerical models are used in different stages in the design of an underground laboratory for radioactive waste disposal.

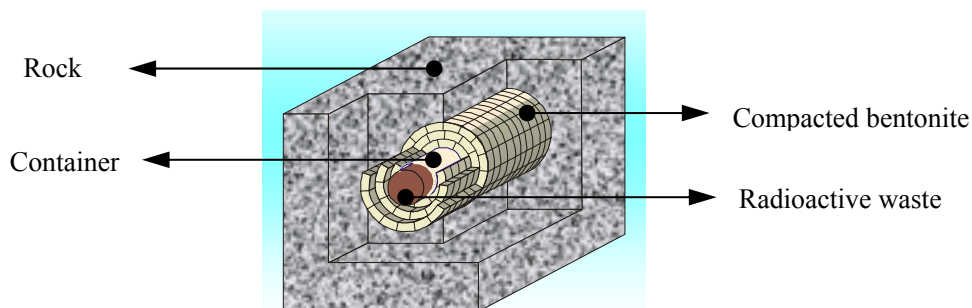


Figure 1. Scheme of the engineered barrier.

During the design of an underground laboratory, scoping calculations reveal useful information related to the expected performance of the barrier under different plausible scenarios. Then, during the operational stage of the experiment, the critical analysis of the comparisons between model outputs and test data is a helpful exercise to understand better the actual *THM* processes. Finally, numerical simulations emerge as indispensable when the interest is focused on performance assessment involving long-term predictions.

Coupled *THM* formulations, and the numerical codes built on them, have been widely used in the design of nuclear waste disposal^{[3],[4],[5]}. A common feature of the approaches cited above is the assumption of the porous medium as a single porosity material and the adoption of average properties over the elementary representative volume. However, in many cases, the low permeability media is characterized by the presence of more than one kind of voids. For instance, in many compacted soils the fabric is composed by an assembly of quasi-saturated aggregates forming a rather open structure that must be distinguished from the clay microstructure itself (Figure 2a). In other cases, the double structure is directly related to the material used, for example in seals composed of high-density pellets with or without powder that fills the pore spaces between them (Figure 2b). Sometimes, the host geological medium can also be considered as a double structure material, for instance, in the case of fractured rock where the distinction between rock matrix and joints is basic to achieve a good representation of the problem. Additionally, the necessity to improve single porosity models can also be found in other fields, such as: in the study of the consolidation in fissured clays, in the exploitation of freshwater-bearing reservoirs, in geothermal system, and in petroleum reservoirs in stratified or fractured media. In all of these cases the inclusion of the different voids levels in the analyses plays a crucial role to a better understanding and explanation of the material behaviour and, evidently, to a proper modelling of these problems.

Therefore, two main objectives have been proposed: the first one is the development of a general *THM* approach for double porosity media and, the second one, is its experimental validation. This work starts with a brief introduction of the proposed double porosity formulation. The main equations of the approach and some aspects of the numerical implementation in the finite element code are presented. Then, a mechanical model specially developed for unsaturated expansive soils is described. Finally, with the aim to validate the double porosity approach, the modelling of an ongoing large-scale heating test is presented.

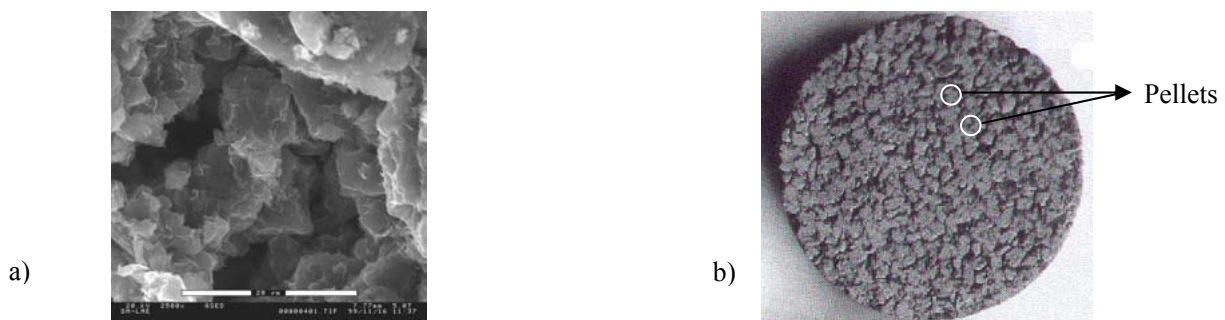


Figure 2. a) Micrograph of a compacted bentonite sample^[2] (dry density = 1.72 Mg/m³). b) Picture of a sample made up of a mixture of clay pellets^[7].

2 THM FORMULATION

A macroscopic approach developed in the context of the continuum theory for porous media is presented herein. The formulation incorporates basic thermal, hydraulic and mechanical phenomena. It is assumed that the porous medium is made up of three phases: solid, liquid and gas. The liquid phase contains water and dissolved air whereas the gas phase is made up of dry air and water vapour.

The problem is approached using a multi-phase, multi-specie formulation that expresses mathematically the main *THM* phenomena in terms of:

- Balance equations.
- Constitutive equations.
- Equilibrium restrictions.

With the aid of the double porosity theory^{[8],[9]}, an existing *THM* formulation for single porosity media^[3] has been extended to media in which two pore structures are present. Double porosity theory considers the porous medium as two interacting continuous media coupled through a leakage term. This term controls the mass transfer between the two porous media. A good schematic representation of the double porosity theory is presented in Figure 3. The fractured porous media is divided into two overlapping but distinct continuum, the first represents flow and deformation in the porous matrix (medium ‘1’) while the second represents flow in the fissures (medium ‘2’). The coupling between both sub-domains is controlled by the leakage term. Medium 1 is composed by the solid and the pores matrix, while medium 2 correspond to the voids of the fractures. A similar conceptual model could be adopted for expansive materials with two different structures of pores. For instance, in the mixture of clays pellets showed in Figure 2b, the medium 1 could be related to the solid particles of the clay pellets and the voids inside the pellets, and the medium 2 could be associated with the macrostructure formed by the pellets (as a whole) and the macropores between pellets.

Porosity, fluids pressures, permeability, degree of saturation and other properties are considered separately for each continuum. It is assumed that two structures of interconnected pores exist, with different properties and fluids that flow through them.

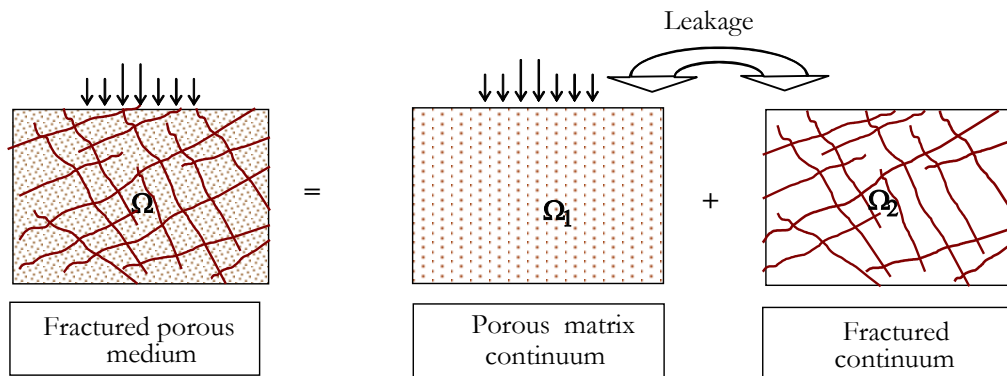


Figure 3. Schematic representation of double porosity concepts^[9].

Some aspects of the formulation are summarized in advance, as follows:

- Two overlapping porous media have been considered, with the definitions of two different global porosities,

$$a) \phi_1 = \frac{V_{v1}}{V}; \quad b) \phi_2 = \frac{V_{v2}}{V}; \quad c) \phi = \phi_1 + \phi_2 \quad (1)$$

where ϕ_1 and ϕ_2 are the porosities related to medium ‘1’ and ‘2’ respectively. ϕ is the global porosity. V_{v1} and V_{v2} are the volume of voids related to each medium and V is the total volume.

- Multiphase, non-saturated flows in each domain are considered.
- Mass transfer processes between media are controlled through leakage terms.
- Stress-small strain constitutive laws can be defined for each porous medium.
- Thermal equilibrium between the phases and the media is assumed.
- The relevant *THM* phenomena are considered in a fully coupled way.

2.1 BALANCE EQUATIONS

The compositional approach has been adopted to establish the mass balance equations. This approach consists of balancing the species (mineral, water and air) rather than the phases (solid, liquid and gas)^[3]. In this way the phase change terms do not appear explicitly, which is particularly useful when equilibrium is assumed. In the notation, the subscript is used to identify the phase (*s* for solid, *l* for liquid and *g* for gas) and the superscript indicates the species: *w* for water and *a* for air. No symbol is attributed to the mineral species, because it has been assumed that it coincides with the solid phase. A second subscript is used to identify the medium (1 or 2). The main balance equations are presented in the following paragraphs, a more detailed description can be found elsewhere^{[6],[10]}.

- Balance of mass of water:

$$\frac{\partial}{\partial t} (\theta_j^w S_j \phi_j + \theta_{gj}^w S_{gj} \phi_j) + \nabla \cdot (\mathbf{j}_{jg}^w + \mathbf{j}_{gj}^w) + (-1)^{j+1} \Gamma^w = f_j^w; \quad j=1,2 \quad (2)$$

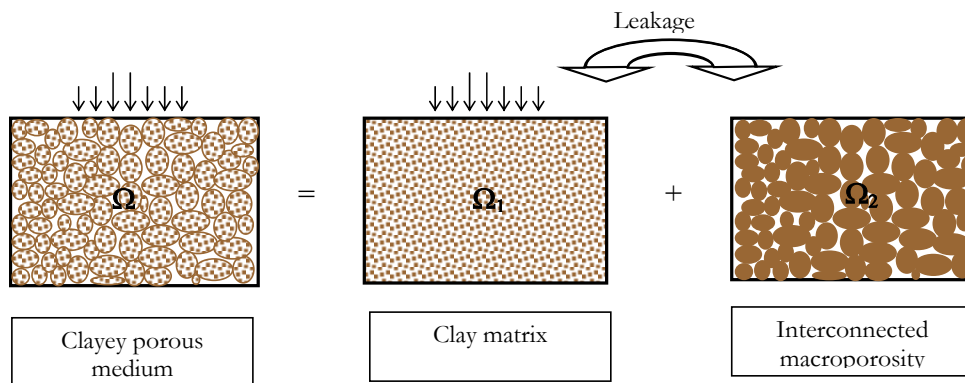


Figure 4. Clayey material, a schematic representation of double porosity concepts.

where θ_{lj}^w and θ_{gj}^w are the masses of water per unit volume of liquid and gas phase respectively. $S_{\alpha j}$ is the volumetric fraction of pore volume occupied by the alpha phase ($\alpha=l,g$). \mathbf{j}_{lj}^w and \mathbf{j}_{gj}^w denote the total mass fluxes of water in the liquid and gas phases with respect to a fixed reference system. f_j^w is the external mass supply of water per unit volume of j medium and Γ^w is the term related to the water mass exchange between the two media, which is explained in Section 2.4.

- Balance of mass of air:

$$\frac{\partial}{\partial t}(\theta_{lj}^a S_{lj} \phi_j + \theta_{gj}^a S_{gj} \phi_j) + \nabla \cdot (\mathbf{j}_{lj}^a + \mathbf{j}_{gj}^a) + (-1)^{j+1} \Gamma^a = f_j^a; \quad j = 1, 2 \quad (3)$$

where θ_{lj}^a and θ_{gj}^a are the masses of air per unit volume of liquid and gas phase respectively. \mathbf{j}_{lj}^a and \mathbf{j}_{gj}^a denote the total mass fluxes of air in the liquid and gas phases with respect to a fixed reference system. f_j^a is the external mass supply of air per unit volume of j medium and Γ^a is related to the mass exchange between media. Note that dry air is considered as a single species in spite of the fact that it is a mixture of gasses. The gaseous phase is assumed as a mixture of air and water vapour. Air is also dissolved in the liquid phase.

- Balance of energy:

$$\begin{aligned} & \frac{\partial}{\partial t} [E_s \rho_s (1-\phi)] + \frac{\partial}{\partial t} \left[\sum_{j=1}^2 (E_{lj} \rho_{lj} S_{lj} \phi_j + E_{gj} \rho_{gj} S_{gj} \phi_j) \right] + \\ & + \nabla \cdot \left[\mathbf{i}_c + \mathbf{j}_{E_s} + \sum_{j=1}^2 (\mathbf{j}_{E_{lj}} + \mathbf{j}_{E_{gj}}) \right] = \sum_{j=1}^2 f_j^E \quad j = 1, 2 \end{aligned} \quad (4)$$

The balance of energy has been expressed in terms of internal energy^{[3],[6]}, where E_s is the solid specific internal energy, E_{lj} and E_{gj} are specific internal energies corresponding to the liquid and gas phases respectively^[6]. ρ_{lj} and ρ_{gj} are the liquid and gas phase densities of the medium. f_j^E is the energy supply per unit volume of medium j . The most important processes for energy transfer in a porous medium have been considered in (4), which are: conduction, advection and phase change^{[3],[6]}. \mathbf{i}_c is the conductive heat flux. \mathbf{j}_s , \mathbf{j}_{El} and \mathbf{j}_{Eg} are the energy fluxes due to the motion of phase.

In this approach a thermal equilibrium between the phases and the media has been assumed, therefore the temperature is the same for the phases and only one equation of total energy is required. This assumption is generally valid in low permeability media. If either the characteristic of the problem or the experimental evidence justifies the necessity of a more detailed treatment of this equation, different temperatures in the two media can be considered.

- Balance of mass of solid:

$$\frac{\partial}{\partial t}(\rho_s (1-\phi)) + \nabla \cdot (\rho_s (1-\phi) \dot{\mathbf{u}}) = 0 \quad (5)$$

where $\dot{\mathbf{u}}$ is the solid velocity vector. The variation of porosities in terms of changes in solid density and volumetric deformation of the soil skeleton is obtained from (5)^{[3],[6]}.

- Balance of momentum (equilibrium):

$$\nabla \cdot \boldsymbol{\sigma}_t + \mathbf{b} = 0 \quad (6)$$

where $\boldsymbol{\sigma}_t$ is the stress tensor and \mathbf{b} the vector of body forces. In (6) inertial terms have been neglected. This assumption is usually accepted because both velocities and accelerations are small, yielding terms that are negligible in comparison with the stress terms. The assumption of small strain rate is also made. Through an adequate constitutive model, the equilibrium equation is transformed into a form expressed in terms of the solid velocities, fluid pressures and temperatures.

Strains are induced by changes in the net stress (total stress minus fluid pressure, see Appendix), suction changes and temperature changes. A possible decomposition of strains is the following:

$$\dot{\boldsymbol{\varepsilon}} = \sum_{j=1,2} \dot{\boldsymbol{\varepsilon}}_j = \sum_{j=1,2} \dot{\boldsymbol{\varepsilon}}_j^e + \dot{\boldsymbol{\varepsilon}}_j^p + \dot{\boldsymbol{\varepsilon}}_j^o; \quad j = 1,2 \quad (7)$$

where $\dot{\boldsymbol{\varepsilon}}_j^e$ is the elastic strain rate due to stress, $\dot{\boldsymbol{\varepsilon}}_j^p$ is the plastic strain rate and $\dot{\boldsymbol{\varepsilon}}_j^o$ identifies generically the strain rate due to changes in fluid pressures or temperature. Deformations due to viscoplastic or creep behaviour can be added in (7). The total strain rate is related with solid velocities through the compatibility conditions, which can be written as:

$$\dot{\boldsymbol{\varepsilon}} = \frac{1}{2} \left(\nabla \dot{\mathbf{u}} + \nabla \dot{\mathbf{u}}^T \right) \quad (8)$$

2.2 CONSTITUTIVE EQUATIONS

The constitutive equations establish the link between the unknowns and the dependent variables. The governing equations are finally written in terms of the unknowns when the constitutive equations are substituted in the balance equations. Here, some of the basic constitutive laws are presented divided in: thermal, hydraulic and mechanical.

- Thermal, heat conduction is assumed to be governed by Fourier's law:

$$\mathbf{i}_t = -\lambda \nabla T \quad (9)$$

where λ is the thermal conductivity of the whole porous medium. More details about the thermal constitutive laws can be found elsewhere^{[6],[10],[11]}.

- Hydraulic, advective fluxes of fluid phase are computed using generalized Darcy's law which is expressed as:

$$\mathbf{q}_{\alpha j} = -\mathbf{K}_{\alpha j} (\nabla P_{\alpha j} - \rho_{\alpha j} \mathbf{g}); \quad \alpha = l, g; \quad j = 1,2 \quad (10)$$

where P_α is the pressure of α phase in the j medium. \mathbf{K}_α is the permeability tensor of α phase in the j medium, computed as:

$$\mathbf{K}_{\alpha j} = \mathbf{k}_j \frac{k_{r\alpha j}}{\mu_{\alpha j}}; \quad \alpha = l, g; \quad j = 1, 2 \quad (11)$$

where \mathbf{k}_j is the intrinsic permeability tensor of medium j , that depends on its pore structure, generally, through the medium porosity (i.e. Table 2). $\mu_{\alpha j}$ is the dynamic viscosity of the α phase in the medium j ^[11]. $k_{r\alpha j}$ is the α phase relative permeability of medium j . A generic expression of $k_{r\alpha}$ in terms of the phase degree of saturation is the following:

$$k_{r\alpha j} = f(S_{\alpha j}); \quad \alpha = l, g; \quad j = 1, 2 \quad (12)$$

The non-advective fluxes of species inside the fluid phases are computed through Fick's law, which expresses them in terms of gradients of mass fraction of species through a hydrodynamic dispersion tensor:

$$\mathbf{i}_{\alpha j}^i = -\mathbf{D}_{\alpha j}^i \nabla \omega_{\alpha j}^i; \quad i = w, a; \quad \alpha = l, g; \quad j = 1, 2 \quad (13)$$

where \mathbf{D}_{α}^i is the dispersion tensor of the medium, and ω the mass fraction of i species in α phase^{[3][6]}. Finally, the retention curve establishes the link between the saturation degree of the medium and the water potential. A well known retention curve is the following^[5]:

$$S_{l_j} = \left(\left(1 + s_j P_0^{-1} \right)^{\frac{1}{1-\lambda_0}} \right)^{-\lambda_0} \left(s_j P_d^{-1} \right)^{\lambda_d}; \quad j = 1, 2 \quad (14)$$

where P_0 , λ_0 , P_d and λ_d are model parameters.

- Mechanical, a *THM* constitutive equation showing explicitly the contributions of strains, temperature and fluid pressures can be expressed generically as:

$$\dot{\boldsymbol{\sigma}}_j = \mathbf{D}_j \dot{\boldsymbol{\varepsilon}}_j + \mathbf{f}_j \dot{s}_j + \mathbf{t}_j \dot{T}_j; \quad j = 1, 2 \quad (15)$$

where $\boldsymbol{\sigma}_j$ is the constitutive stress (net or effective stress), $\boldsymbol{\varepsilon}_j$ is the strain vector, s_j is the media suction ($p_g - p_{lj}$), \mathbf{D}_j is the constitutive stiffness matrix, \mathbf{f}_j is the generic constitutive vectors relating the changes in the fluid pressures and stresses and \mathbf{t}_j is the constitutive vector relating stresses and temperature. Different mechanical laws can be incorporated to describe the material behaviour. In Section 4, a mechanical model for expansive materials is presented.

2.3 EQUILIBRIUM RESTRICTIONS

It is assumed that phase changes are rapid in relation to the characteristic times typical of the problems in low permeability media. Therefore, they can be considered in local equilibrium giving rise to a set of equilibrium restrictions that must be satisfied at all times. This implies that the species concentration in the various phases can be considered as dependent variables. Equilibrium restrictions are given by the concentration of water vapour in gas phase, which is computed through the psychometric law; and by the concentration of dissolved air in liquid phase, which is evaluated by means of Henry's law^{[5],[6],[10]}.

2.4 MASS TRANSFER BETWEEN MEDIA

In (2) and (3) the term Γ^i ($i=w,a$) controls the mass transfer between media. A simple model for this term can be expressed as:

$$\Gamma^i = \gamma(\Psi_1 - \Psi_2) \quad (16)$$

where γ is the leakage parameter and Ψ_j ($j=1, 2$) represents the variable involved in the mass transfer. When water mass transfer is considered, the total water potential is the variable involved in (16). In some cases variables related to the total water potential are adopted as main responsible of the mass transfer process. Generally the fluid pressures are the variable adopted to model the mass transfer between media. This is the variable adopted in this work.

In (16) it is assumed that the process of mass transfer has reached a quasi-steady state^[12]. A more refined treatment of this term can be made through the unsteady models^[12]. In these models the transfer of mass between media is obtained solving the 1-D diffusion problem for an idealized geometry of the matrix pores^{[6],[12]}. In this formulation the two kinds of models can be potentially used, the selection will depend on the characteristic of each problem.

3 NUMERICAL IMPLEMENTATION

The mass balance equations presented above (2) to (5) are transformed algebraically in a more convenient form for programming purpose^[6]. The final form of the water mass balance equation is presented as an example:

$$\begin{aligned} \phi_j \frac{\partial}{\partial t} (\theta_{lj}^w S_{lj} + \theta_{gj}^w S_{gj}) + (\theta_{lj}^w S_{lj} + \theta_{gj}^w S_{gj}) \left[\left(\frac{(1-\phi)}{\rho_s} \frac{\partial \rho_s}{\partial t} \right)^{(2-j)} + \dot{\epsilon}_{vj} \right] + \\ + \nabla \cdot (\mathbf{j}_{lj}^w + \mathbf{j}_{gj}^w) + (-1)^{j+1} \Gamma^w = f_j^w \quad j = 1, 2 \end{aligned} \quad (17)$$

The other balance equations have been considered in a similar way^[6]. The numerical treatment of the different terms involved in the mass balance equations has been made as it is explained in Olivella et al.^[13]. One unknown (state variable) is associated with each of the mass balance equations presented. For the more general case the unknowns are the following: velocity field, fluid pressures (gas and liquid pressures) and temperature. The unknowns are obtained by solving the system of PDE's (Partial Differential Equations) numerically in a fully coupled way. From state variables, dependent variables are calculated using the constitutive equations or the equilibrium restrictions.

The formulation has been implemented^[6] in CODE_BRIGHT^{[11],[13]}, a 3-D finite element program. The numerical approach can be viewed as divided into two parts: spatial and temporal discretization. Galerkin finite element method is used for the spatial discretization while finite differences are used for the temporal discretization. The discretization in time is linear and an implicit scheme has been used. The program has an automatic discretization of time. The Newton-Raphson method has been adopted as iterative scheme to solve the non-linear problem. More details related to the CODE_BRIGHT program can be found in^{[11],[13]}.

4 MECHANICAL CONSTITUTIVE MODEL FOR EXPANSIVE CLAYS

The application case presented in this work is related to the analysis of coupled *THM* processes in a clay barrier. Thus, some aspects of the swelling clay behaviour are summarized below. The mechanical constitutive law is a key element in the modelling of swelling clays owing to the strong influence of the mechanical problem on the behaviour of these clays. A crucial aspect to understand and reproduce properly the behaviour of swelling clays is the inclusion of the clay fabric effects in the analysis^[14]. Sánchez et al.^[15] presents a mechanical model for expansive clays based on the approach proposed by Gens & Alonso^[14]. A fundamental characteristic of the framework is the explicit distinction of two structural levels within the material: the macrostructure, which accounts for the larger scale structure of the material and the microstructure, associated to the active clay responsible for the swelling behaviour. The model also contemplates the interaction between both structural levels^{[14],[15]}.

These two basic structural levels actually exist in many expansive soils. For instance, Figure 5a, shows the results of mercury intrusion porosimeter tests of FEBEX bentonite (Figure 2b), in which a clear bimodal pore distribution (characteristic of the expansive clays) can be observed. The dominant values are 10 nm that would correspond to the pores inside clay aggregates. On the other hand, a larger pore size, which depends on the compaction dry density, ranges from 10 μm and 40 μm . The boundary between the two pore size families is around 130 nm. These two dominant pores size could be associated with the two basic structural levels mentioned above: the macro structure (medium 2) and micro structure (medium 1). Figure 5b presents a schematic representation of the conceptual model.

The complex behaviour exhibited by expansive materials under different *THM* conditions requires the development of non-standard models that contemplate the main observed trend. The model presented herein has been formulated using concepts of elasto-plasticity for strain hardening materials. The mathematical framework used to formulate the model is presented in detail in^{[6],[15]}. The Appendix contains the main model equations. The model is formulated in terms of the three stress invariants (p , J , θ), suction (s) and temperature (T). The complete model formulation requires the definition of laws for: i) the macrostructural level, ii) the microstructural level and iii) the interaction between both structural levels. These laws are briefly introduced in the following sections.

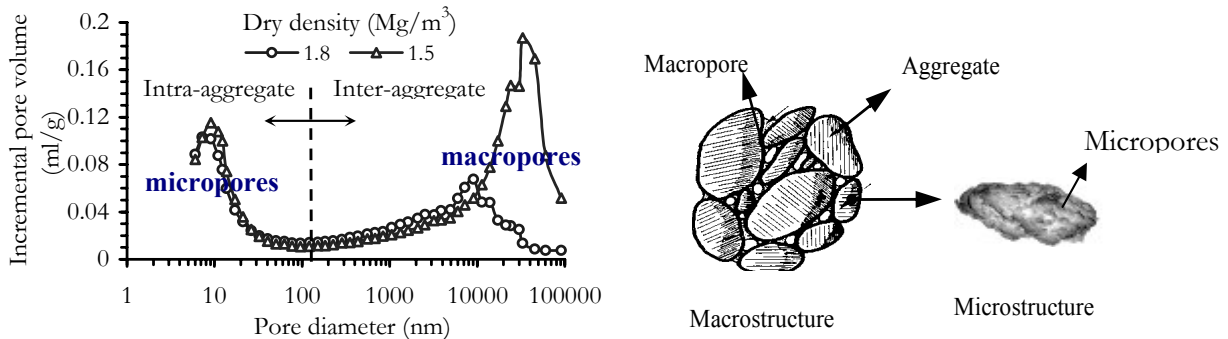


Figure 5. a) Distribution of incremental pore volume for two compacted bentonite samples at different dry densities^[2]. b) Schematic representation of the two structural levels considers.

4.1 MACROSTRUCTURAL MODEL

The inclusion of this structural level in the analysis allows the consideration of phenomena that affect the skeleton of the material, for instance deformations due to loading and collapse. These phenomena have a strong influence on the macroscopic response of expansive materials. The macrostructural behaviour can be described by concepts and models of unsaturated non-expansive soils, such as the elasto-plastic Barcelona Basic Model (*BBM*)^[16]. The *BBM* considers two independent stress variables to model the unsaturated behaviour: the net stress ($\boldsymbol{\sigma}$) computed as the excess of the total stresses over the gas pressure ($\boldsymbol{\sigma}_r - \mathbf{I}p_g$), and the matric suction (s_2). The *BBM* extends the concept of critical state to the unsaturated conditions. The *BBM* yield surface (Figure 6a) depends not only on the stress level and on the history variables (as in a critical state model) but also on the matric suction. The *BBM* yield surface (F_{LC}) is given by^[15]:

$$F_{LC} = 3J^2 - \left[\frac{g(\theta)}{g(-30^\circ)} \right]^2 M^2 (p + p_s)(p_o - p) = 0 \quad (18)$$

where M is the slope of the critical state, p_o is the apparent unsaturated pre-consolidation pressure, $g(\theta)$ is a function of the lode angle, p is the net mean stress and p_s considers the dependence of shear stress on suction and temperature. A basic point of the model is that the size of the yield surface increases with suction. The trace of the yield function on the isotropic p - s plane is called *LC* (Loading-Collapse) yield curve, because it represents the locus of activation of irreversible deformations due to loading increments or collapse (when the suction reduces). The position of the *LC* curve is given by the pre-consolidation yield stress of the saturated state, p_o^* , (hardening variable), according to the following expression^[15]:

$$\dot{p}_o^* = \dot{p}_o^* \frac{(1+e)}{(\lambda_{(0)} - \kappa)} \dot{\varepsilon}_v^p \quad (19)$$

where e is the total void index, $\dot{\varepsilon}_v^p$ is the volumetric plastic strain, κ is the elastic stiffens parameter for changes in p and $\lambda_{(0)}$ is the stiffness parameter for changes in p for virgin states of the soil in saturated conditions. The inclusion of the thermal effects has been made according to Gens^[17]. In this way it is considered that temperature increases reduce the size of the yield surface and the strength of the material.

4.2 MICROSTRUCTURAL MODEL

The microstructure is the seat of the basic physical-chemical phenomena occurring at clay particle level, which are basically reversible. These phenomena are the main responsible of the expansive soils behaviour. The microstructural effective stress is defined as^[15]:

$$\hat{p} = p + \chi s_t; \quad s_t = s_2 + s_o \quad (20)$$

where s_o is the osmotic suction, s_t is the total suction and χ is a constant ($\chi > 0$).

The effect of the osmotic suction is not considered in this work; therefore, it is assumed that the total suction is equal to the matric suction (s_2). In Guimarães et al.^[17] the model has been extended to include the effect of the osmotic suction and cation exchange. In (20) hydraulic equilibrium between the water potentials of both structural levels has been assumed (i.e. $s=s_I=s_2$). The extension of the constitutive model to handle problems in which this hypothesis is released is presented in Sánchez^[6].

In the p - s plane the line corresponding to constant microstructural effective stresses is referred to as Neutral Line (NL), since no microstructural deformations occur when the stress path moves on it (Figure 6b). The deformations arising from microstructural phenomena are considered elastic and volumetric and are obtained as:

$$\dot{\varepsilon}_{v_1}^e = \frac{\dot{\hat{p}}}{K_1} = \frac{\dot{p}}{K_1} + \chi \frac{\dot{s}}{K_1} \quad (21)$$

where the superscript e refers to the elastic component of the volumetric (subscript v) strains and K_1 is the microstructural bulk modulus.

According to (21) the Neutral Line divides the p - s plane into two parts (Figure 6b), defining two main generalized stress paths, which are identified as:

$$\dot{\hat{p}} > 0 \Rightarrow \text{microstructural contraction (MC)} ; \quad \dot{\hat{p}} < 0 \Rightarrow \text{microstructural swelling (MS)}$$

4.3 INTERACTION BETWEEN STRUCTURAL LEVELS

In expansive soils there are other mechanisms in addition to the ones included in the BBM which induce plastic strains. This irreversible behaviour is ascribed to the interaction between the macro and micro structures^{[14],[15]}. Observing the behaviour of expansive clays in cycles of suction reversals, two main aspects can be highlighted: i) the irreversible behaviour appears independently of the applied suction and ii) it is difficult to determine the initiation of the yielding. These facts aim the use of the generalized plasticity theory to formulate the model.

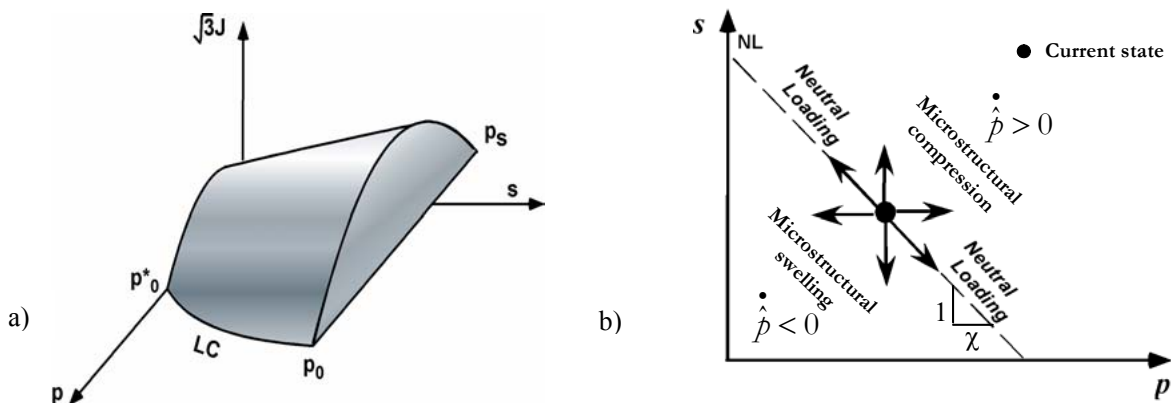


Figure 6. a) Three dimensional representation of the BBM yield surface. b) Definition of microstructural swelling and contraction directions on the p - s plane.

In a generalized plasticity model the yield function is not defined or it is not defined in an explicit way^{[19],[15]}. Some of the advantages in using the generalized plasticity theory to model the plastic mechanism related to the interaction between both pores structures are:

- No clear evidence exists concerning the shape of the internal yield surfaces corresponding to the interaction mechanisms between the two structural levels. Furthermore, their experimental determination does not appear to be easy either.
- The effect of drying/wetting cycles on the behaviour of expansive soils is a matter of great practical importance. Generalized plasticity is especially well adapted to deal with cyclic loading^{[19],[15]}.
- It provides sufficient flexibility to incorporate additional microstructural phenomena such as non-equilibrium microstructural suction^[6], or geochemical variables such as osmotic suction and cation exchange^[17].

Moreover, in the case that the yield surfaces related to this mechanism can be experimentally defined, there are no problems to include them in the modelling, since the classical plasticity theory is a particular case of the generalized plasticity^[19].

An assumption of model is that the irreversible strains of the macrostructure are proportional to the microstructural strains according to interaction functions f ^{[14][15]}. This plastic macrostructural strains are computed by the following expression:

$$\dot{\boldsymbol{\varepsilon}}_{v2}^p = f \dot{\boldsymbol{\varepsilon}}_{v1}^e \quad (22)$$

Two interaction functions f are defined: f_c for microstructural contraction paths and f_s for microstructural swelling paths. The interaction function depends on the ratio p/p_o (p_o is the net mean yield stress at current suction and temperature). This ratio is a measure of the degree of openness of the macrostructure^[14]. The coupling between both plastic mechanisms is considered mathematically assuming that^[15]:

$$\dot{\boldsymbol{\varepsilon}}_v^p = \dot{\boldsymbol{\varepsilon}}_{vLC}^p + f \dot{\boldsymbol{\varepsilon}}_{v1} \quad (23)$$

where $\boldsymbol{\varepsilon}_{vLC}^p$ is the plastic strains induced by the yielding of the macrostructure (*BBM*). The coupling is given by p_o^* , hardening variable of the macrostructure (Figure 6a), which depends on the total plastic volumetric strain (19). In this way is considered that microstructural effects can affect the global arrangements of aggregates (macrostructure).

Note that the material response will depend strongly on the direction of the microstructural stress path, being the *NL* which delimits two regions of different material behaviour. In order to describe correctly the material behaviour, the definition of specific elasto-plastic laws for each domain is required according to the microstructural stress path followed (*MC* or *MS*). The generalized plasticity theory can deal with such conditions, allowing the consideration of two directions of different behaviour and the formulation of proper elasto-plastic laws for each region. A complete model description includes the definition of the: i) loading and unloading direction, ii) plastic flow direction, and iii) a plastic modulus. Details of the model formulation can be found in Sanchez^[6] and Sanchez et al.^[15].

In summary, the behaviour of the macrostructure is modelled in the context of classical plasticity (*BBM*). This is a proper framework because the yield surface associated to this behaviour could be generally inferred by the usual methodology of classic plasticity. The microstructural effects have been modelled using a nonlinear elastic model. The interaction between pores structures has been model using the more general framework of generalized plasticity theory. Finally, the governing small strain-stress equations have been obtained using a general framework for multidissipative materials^[15].

A critical step in the implementation of a mechanical model in a finite element program is the development of a proper algorithm to update the stresses and the internal variables of the model. Since the stresses should be integrated many times on the course of a typical nonlinear simulation, the selection of the algorithm has been based on the accuracy of the solution and also on its robustness and efficiency. The numerical integration of the model has been performed using a refined Euler scheme with automatic sub-stepping and error control^[6]. The algorithm is an adaptation of the scheme proposed by Sloan^[20] to the specific characteristics of this model^[6]. A great advantage of Sloan's schemes is that they have been widely tested in geotechnical problems, evincing their accuracy, robustness and efficiency.

5 APPLICATION

The proposed approach has been used to analyze several engineering problems involving coupled *THM* processes in geological media^[6]. The applications have been mainly focused on the study of the coupled *THM* phenomena in engineered clay barriers and seals. However, the suggested formulation is general and it is not limited to study problems in which expansive materials are involved. For instance, the problem of consolidation in fissured clays or the simulations of petroleum exploitations in stratified media have also been analyzed^[6]. A good performance of the double porosity formulation has been observed in the cases studied.

The experimental validation of the formulation has been mainly supported by the data generated in the framework of the FEBEX (Full-scale Engineered Barriers Experiment) project^[21]. The main aim of the FEBEX project is the study of the engineered barrier and the near field components of a high level radioactive waste disposal. The experimental part of the project is made-up of three main components: i) an *in-situ* test (under natural conditions and at full scale); ii) a *mock-up* test (under laboratory conditions at almost full scale) and, iii) a series of laboratory tests to complete the information from the two large-scale tests. The data of laboratory tests have been used to identify the main parameters of the constitutive laws related to the thermal, hydraulic and mechanical problems. The large scale heating tests (*in-situ* and *mock-up* tests) have allowed the application of the approach to actual cases in which experimental information of the main *THM* variables are available.

This work presents some results of the *mock-up* test modelling. The experiment (Figure 7) is being carried out in the CIEMAT laboratory (Madrid). Two electrical heaters (simulating canisters containing heat-emitting waste) are placed in the centre of a steel cylinder 6 m long and with inner diameter of 1.62 m.

The space between heaters and steel cylinder is filled with a 0.64 m-thick engineered barrier made up of compacted FEBEX bentonite (the final global dry density of the clay barrier is 1.65 Mg/m^3) The barrier is hydrated uniformly form all around the cylinder with an applied water pressure of about 0.5 MPa. Simultaneously, the barrier is heated maintaining a constant temperature of $100 \text{ }^\circ\text{C}$ in the contact between heaters and bentonite. The laboratory temperature is also controlled ($\approx 20 \text{ }^\circ\text{C}$). The test is very well instrumented, with several sensors located along the barrier which register the evolution of the main *THM* variables^[21]. The *mock-up* test avoids many of the uncertainties arising form the natural system. This is achieved mainly due to the good control of the initial and boundary conditions of the test.

The *THM* behaviour of the heating test has been successfully modelled during the operational stage of the experiment^{[6],[21],[22]}. *THM* coupled analyses have been performed using 1-D axisymetric models and 2-D axisymetric longitudinal section^{[21][22]}. In this case only one half of the problem is analyzed because of symmetry. The unknowns of the problem are: displacement field, fluid pressures and temperature. The most advanced numerical analysis performed corresponds to the double structure model developed using the framework presented in the previous sections. The use of this approach is required due to the clear dual porosity of the FEBEX bentonite (Figure 5a). An advantage of this model is the possibility to include the clay fabric effects in the *THM* modelling, which is a crucial aspect in this kind of analysis^{[1],[6]}. The parameters of the thermal, hydraulic and mechanical constitutive laws have been obtained^{[2],[6],[21],[22]} from the experimental data generated in the context of the FEBEX project. Tables 1 to 3 present the model parameters adopted in this simulation and Figure 8 shows the global retention curve of the medium together with the experimental data at different dry densities of the FEBEX bentonite^[21].

The physical processes involved in the *THM* behaviour of a clay barrier are discussed in detail in other contributions^{[4],[5],[6]}. A summary of the main trend observed in the thermal, hydraulic and mechanical problems is presented in the following paragraphs.

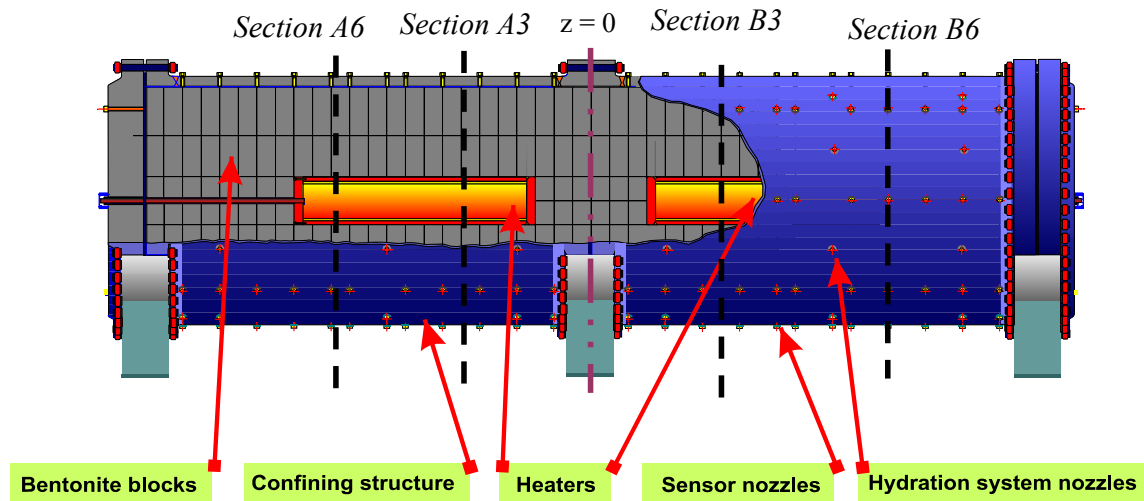


Figure 7. Layout of the large scale heating test.

Table 1. Thermal constitutive law^{[21],[6]}

Parameters defining the thermal conductivity: $\lambda = \lambda_{sat}^{S_l} \lambda_{dry}^{(1-S_l)}$, $S_l = \frac{S_{l1} \phi_1 + S_{l2} \phi_2}{\phi}$	
λ_{sat} (W/m°C) = 1.15	λ_{dry} (W/m°C) = 0.47

Table 2. Mechanical constitutive laws^{[2],[6]}

Parameters defining the Barcelona Basic Model for macrostructural behaviour							
κ	κ_s	$\lambda_{(o)}$	p_c (MPa)	r	ζ (MPa ⁻¹)	p_o^* (MPa)	α_0 (°C ⁻¹)
0.007	0.001	0.080	0.50	0.90	0.20	5.4	$1.5 e^{-05}$
Parameters defining the law for microstructural behaviour							
α_m (MPa ⁻¹) = $2.1 e^{-02}$				β_m (MPa ⁻¹) = $2.0 e^{-03}$			
Interaction functions							
$f_c = 1 + 0.9 \tanh(20(p/p_o) - 0.25)$; $f_s = 0.8 - 1.1 \tanh(20(p/p_o) - 0.25)$							
Void ratio							
$e_{macro} = 0.196$				$e_{micro} = 0.45$			

Table 3. Hydraulic constitutive laws^[6]

Parameters defining the permeability laws: $k_j = k_{0j} \exp[b(\phi - \phi_0)] I$; $k_{r,j} = (S_{l,j})^n$; $k_{rg,j} = (1 - k_{r,j})$				
$k_{0,1}$ (m ²)	$k_{0,2}$ (m ²)	ϕ_0	b	n
$5.0 e^{-20}$	$5.0 e^{-23}$	0.14	50	1
Leakage parameter $\gamma = 1.0$ (kg s ⁻¹ m ⁻³ MPa ⁻¹)				

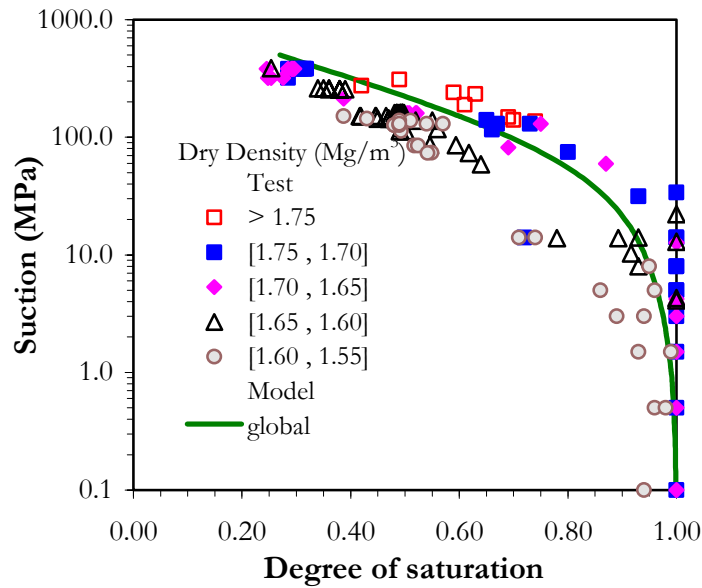


Figure 8. Water retention curve and experimental data.

5.1 THERMAL PROBLEM

An initial temperature of 20 °C has been assumed. A constant temperature of 100 °C has been fixed in the contact between heater and bentonite. The model yields good results regarding the thermal problem. This is reflected either in the evolution of the temperature in different points of the barrier (Figure 9) or in the evolution of the power emitted by the heaters (which is a global variable of the problem), as it is showed in Figures 10. From this figures it can be observed that the global tendency of the test is well capture by the model.

5.2 HYDRAULIC PROBLEM

An average relative humidity close to 47 % has been registered before the hydration of the test, so, an initial suction of 105 MPa has been adopted. The initial water content of the clay is 14%. According with the test conditions, a constant liquid pressure of 0.5 MPa has been fixed in the periphery. Figure (11) shows that the model offers a good reproduction of the total water entry in the test. Figure (12) presents the time evolution of the relative humidity in different radii of the barrier. The overall behaviour of the experiment is the expected one, that is: in zones close to the hydration front it can be observed an increasing saturation from the beginning of the test, while in regions close to the heaters it can be observed an intense drying just after the start of the heating phase, followed by a slow hydration as times goes on. The behaviour of zones close to a radius of 0.37m shows an initial wetting, due to the condensation of the water vapour coming form the inner region, then a drying due to heating and finally a progressive wetting. Similar behaviour has been observed in other sections of the test^{[21][22]}. A non-planned overheating episode, which took on the day 1391 of the test, had a strong influence in the normal evolution of the test (Figure 12).

5.3 MECHANICAL PROBLEM

A hydrostatic value of 0.11 MPa has been adopted for the initial stress state, approximately equal to the weight of the bentonite in the mid diameter of the buffer. A stress free outer boundary has been prescribed. Satisfactory results have also been obtained in terms of stresses. For instance, Figure 13 presents the evolution of radial stress for two representative sections of the test. It can be observed the strong influence that the overheating event had over the evolution of stresses. A detailed explanation of this event and the *THM* modelling it can be found in Sánchez et al.^[15].

6 CONCLUSIONS

The availability of a coupled formulation that expresses, in a mathematical way, the various thermo-hydro-mechanical phenomena deemed relevant and their mutual interactions is a basic requirement for a good understanding and representation of complex *THM* problems.

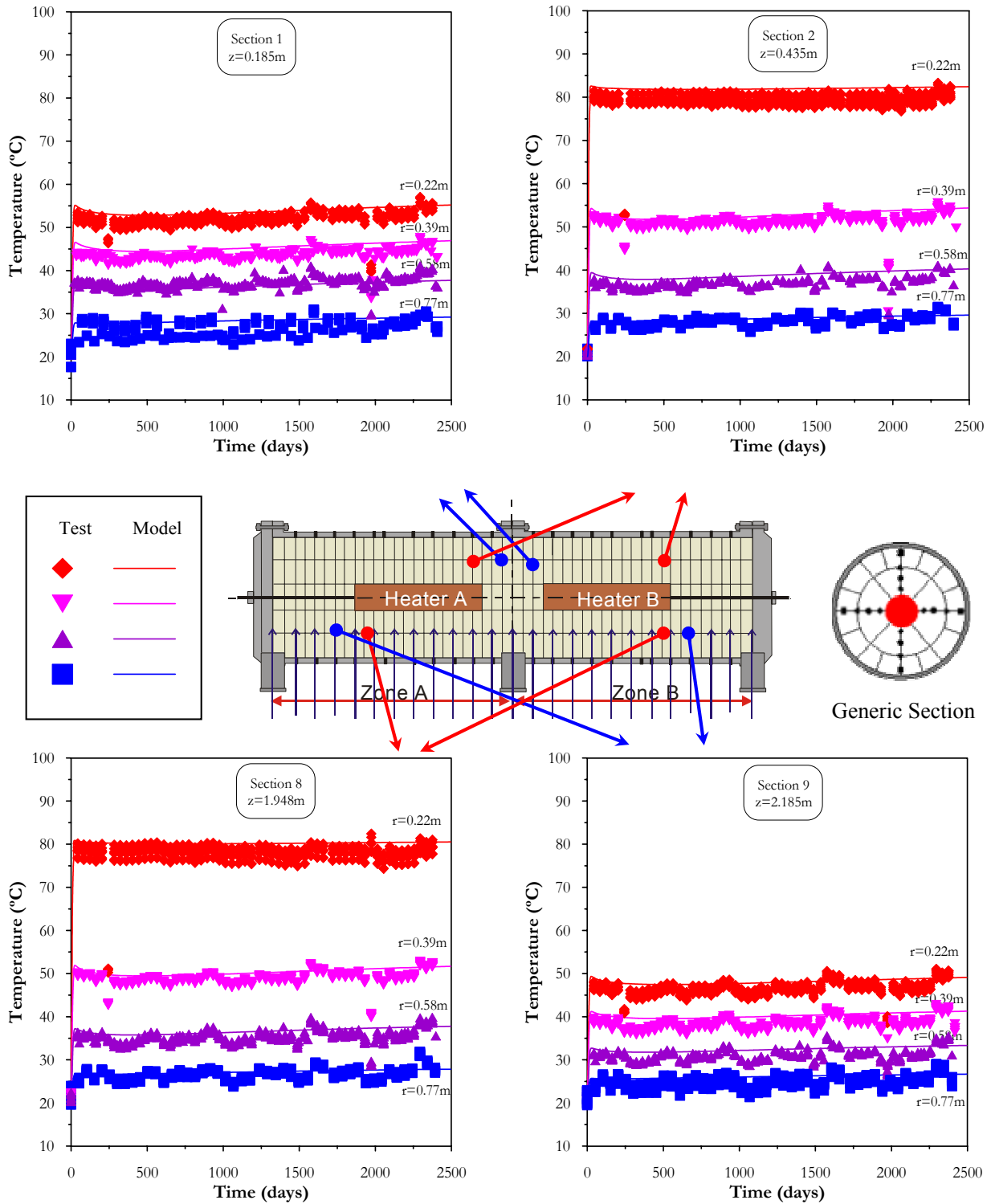


Figure 9. Evolution of temperature in the *mock-up* test in different sections and at different radii (r). Observed versus computed values.

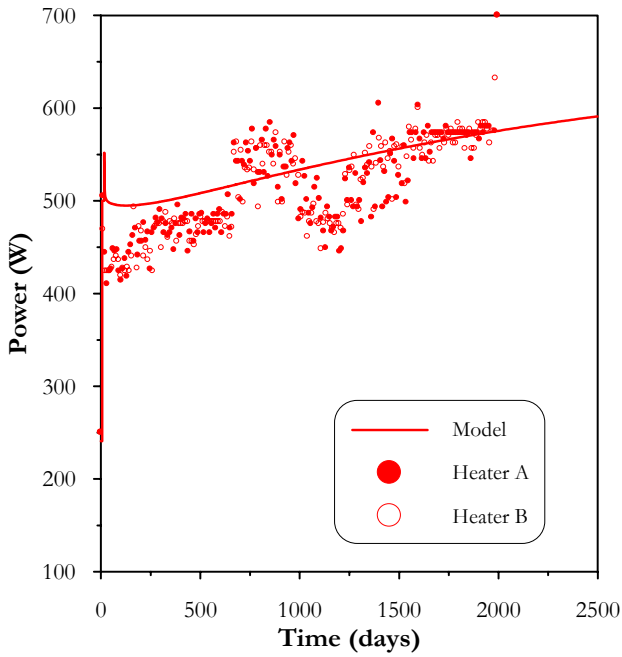


Figure 10. Evolution of heater power in the *mock-up* test. Observed and computed values.

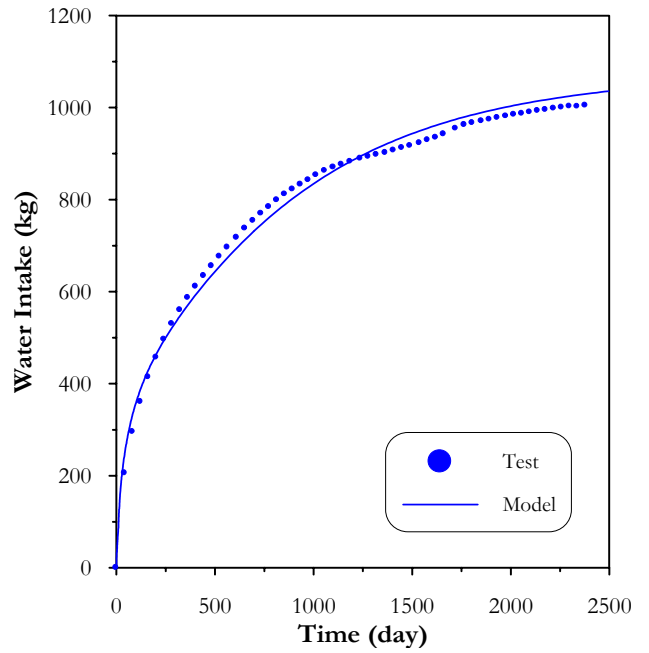


Figure 11. Evolution of the total water intake in the *mock-up* test. Observed and computed values.

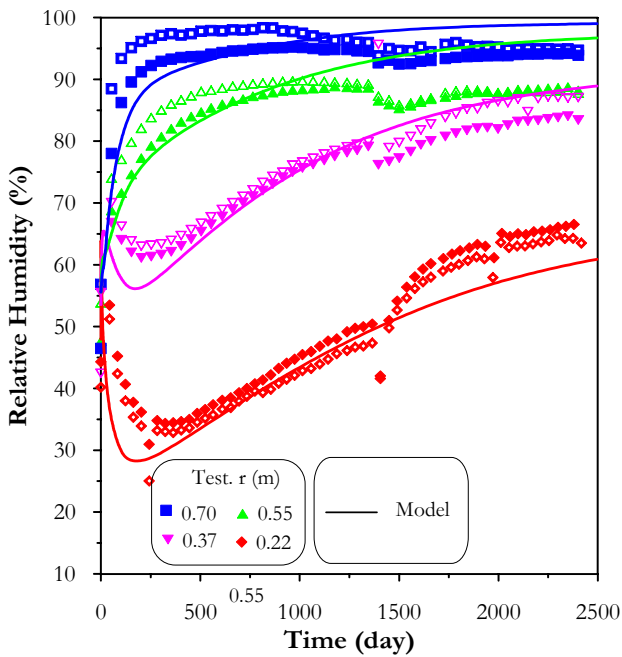


Figure 12. Evolution of relative humidity in the *mock-up* test. Observed and computed values.

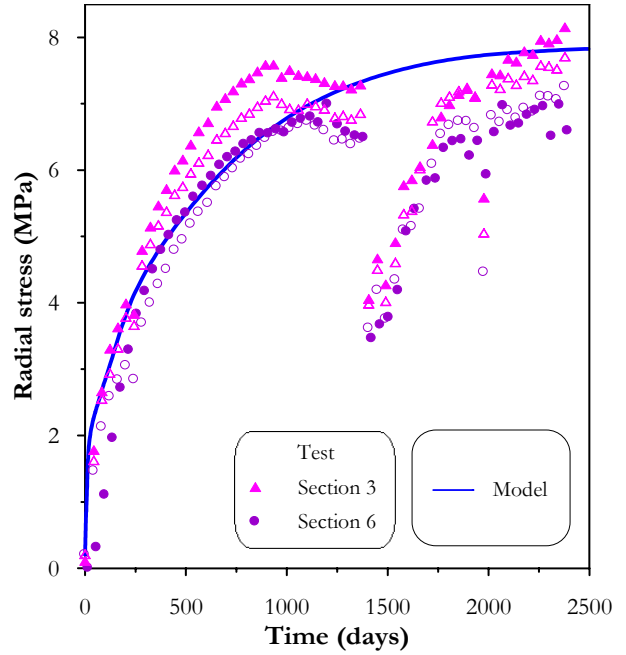


Figure 13. Evolution of radial stress in the *mock-up* test. Observed and computed values.

A coupled *THM* framework for porous media with two distinctive types of voids has been presented in this work. Special attention has been placed on the formulation of the constitutive model for expansive materials, which is a key element in the modelling of the swelling clay behaviour. In order to be closer to the typical fabric of expansive materials the existence of two pores structures has been explicitly included in the model. The approach has been implemented in a finite element code allowing the incorporation of these concepts in the numerical analyses readily. Finally, the formulation has been used to model an ongoing large scale heating test in which the fabric of the material presents a clear double porosity. The proposed approach is adequate for the analysis of these kind of problems, since not only the relevant physical phenomena are captured but also satisfactory quantitative agreements with measurements are obtained.

7 ACKNOWLEDGEMENTS

The authors would like to acknowledge ENRESA (Spanish national company for radioactive waste, S.A.) for funding this work. The project FEBEX is partially funded by the European Commission.

8 REFERENCES

- [1] Y. Cui, C. Loiseau & P. Delage. "Water transfer through a confined heavily compacted swelling soil". *6th International Workshop on Key Issues in Waste Isolation Research; Proc. Symp. Paris, November 2001*, 43-60 (2001).
- [2] A. Lloret, M.V. Villar, M. Sánchez, A. Gens, X. Pintado, & E. Alonso. "Mechanical behaviour of heavily compacted bentonite under high suction changes". *Géotechnique*, **53**(1), 27-40 (2003).
- [3] S. Olivella, J. Carrera, A. Gens & E. Alonso. "Non-isothermal multiphase flow of brine and gas through saline media". *Transport in porous media*, **15**, 271-293 (1994).
- [4] H.R. Thomas & Y. He. An analysis of coupled heat, moisture and air transfer in a deformable unsaturated soil". *Géotechnique*, **45**, 667-689 (1995).
- [5] A. Gens, A. Garcia Molina, S. Olivella, E. Alonso & F. Huertas. "Analysis of a full scale in-situ test simulating repository condition". *Int. Jnl. Numer. Anal. Meth. In Geomech.*, **22**, 515- 548 (1998).
- [6] M. Sánchez. *Thermo-hydro-mechanical coupled analysis in low permeability media*. Ph. D. Thesis, Technical University of Catalonia. Barcelona (2004)
- [7] E. Alonso & J. Alcoverro. *Calculation and testing of behaviour of unsaturated clay as barrier in radioactive waste repositories*. Tech. public. 11/99. Madrid: ENRESA (1999).
- [8] E. Aifantis. "On the problem of diffusion in solids". *Acta Mechanica* **37**(3-4), 265-296 (1980).
- [9] H. Ghafouri & R. Lewis. "A finite element double porosity model for heterogeneous deformable porous media". *Int. Jnl. Numer. Anal. Meth. Geomech* **20**, 831- 844 (1996).
- [10] M. Sánchez, S. Olivella & A. Gens. "A coupled double structure *THM* formulation". *Int. Jnl. Numer. Anal. Meth. In Geomech.* (in revision).

- [11] *CODE_BRIGHT User's Manual*. UPC Geomechanical Group (2004)
- [12] B. Huyakorn, Lester & C. Faust. "Finite element techniques for modelling groundwater flow in fractured aquifers". *Water Resources Research*, **19**(4), 1019-1035 (1983).
- [13] S. Olivella, A. Gens, J. Carrera & E. Alonso. "Numerical formulation for a simulator (CODE-BRIGHT) for the coupled analysis of saline media". *Engineering Computations*, **13**(7), 87-112 (1996).
- [14] A. Gens & E. Alonso. "A framework for the behaviour of unsaturated expansive clays". *Can. Geotech. Jnl.* **29**, 1013-1032 (1992).
- [15] M. Sánchez, A. Gens, L. Guimarães & S. Olivella "A double structure generalized plasticity model for expansive materials". *Int. Jnl. Numer. Anal. Meth. In Geomech.* (accepted).
- [16] E. Alonso, A. Gens & A. Josa. "A constitutive model for partially saturated soils". *Géotechnique*, **40**(3), 405-430 (1990).
- [17] A. Gens. "Constitutive Laws". *Modern issues in non-saturated soils*, A. Gens, P. Jouanna & B. Schrefler (ed.). Springer-Verlag, 129-158 (1995).
- [18] L. Guimarães, A. Gens, M. Sánchez, & S. Olivella. "Chemo-mechanical modelling of expansive materials". *6th International Workshop on Key Issues in Waste Isolation Research; Proc. Symp. Paris, November 2001*, 463-495 (2001).
- [19] M. Pastor, O. Zienkiewics, & A. Chan. "Generalized plasticity and the modelling of soil behaviour". *Int. Jnl. Numer. Anal. Meth. Geomech.* **14**, 151-190 (1990).
- [20] S. Sloan, A. Abbo & D. Sheng. "Refined integration of elastoplastic models with automatic error control". *Engineering Computation*, **18** (1/2), 121-154 (2001).
- [21] FEBEX Project. *Full-scale engineered barriers experiment for a deep geological repository for high level radioactive waste in crystalline host rock. Final project report*. EUR 19612 EN, European Commission, Brussels (2000).
- [22] M. Sánchez & A. Gens. *Second report on THM modelling results. FEBEX II*. UPC Geomechanical Group. ENRESA Report: 70-UPC-L-5-011 (2002).

APPENDIX. MECHANICAL MODEL

A detailed description of the mechanical model can be found in^{[6],[15]}. The *BBM* yield surface (F_{LC}) is given by (18) and the plastic potential (G) is expressed as:

$$G = \alpha 3J^2 - \left[\frac{g(\theta)}{g(-30^\circ)} \right]^2 M^2 (p + p_s)(p_0 - p) = 0 \quad (\text{A1})$$

where α is determined according to^[16].

The dependence of the tensile strength on suction and temperature is given by:

$$p_s = k_s e^{-\rho \Delta T} \quad (\text{A2})$$

where k and ρ are model parameters.

The dependence of p_0 on suction is given by:

$$\dot{p}_0 = p_c \left(\frac{\dot{p}_{0T}^*}{p_c} \right)^{\frac{\lambda_{(s)} - \kappa}{\lambda_{(s)} - \kappa}}; \quad \dot{p}_{0T}^* = \dot{p}_0^* + 2\alpha_1 \Delta T \quad (\text{A3})$$

where p_c is a reference stress and α_l is a model parameter. $\lambda_{(s)}$ is the stiffness parameter for changes in net mean stress for virgin states of the soil at the given suction s_l , this parameter depends on suction according to:

$$\lambda_{(s)} = \lambda_{(0)} [r + (1-r) \exp(-\zeta s)] \quad (\text{A4})$$

where r is a parameter which defines the maximum soil stiffness and ζ is the parameter which controls the rate of increase of soil stiffness with suction.

The stress invariants are evaluated as follows:

$$\dot{p} = \frac{1}{3} (\dot{\sigma}_x + \dot{\sigma}_y + \dot{\sigma}_z); \quad J^2 = 0.5 \operatorname{tr}(\mathbf{s}^2); \quad \theta = -\frac{1}{3} \sin^{-1} (1.5\sqrt{3} \det \mathbf{s} / J^3) \quad (\text{A5})$$

$$\text{where: } \mathbf{s} = \boldsymbol{\sigma} - p\mathbf{I}; \quad \boldsymbol{\sigma} = \boldsymbol{\sigma}_t - \mathbf{I}p_f \quad (\text{A6})$$

$$\text{and: } p_f = p_g \quad \text{if } p_g > p_l; \quad \text{otherwise } p_f = p_l$$

The macrostructural bulk modulus (K_1) for changes in mean stress and the microstructural bulk modulus (K_2) are evaluated with the following laws:

$$K_1 = \frac{e^{-\alpha_m \dot{p}}}{\beta_m}; \quad K_2 = \frac{(1+e_2)}{\kappa} p \quad (\text{A7})$$

where α_m and β_m are model parameters.

The shear modulus G_t is obtained from a linear elastic model as follows:

$$G_t = \frac{3(1-2\mu)K}{2(1+\mu)} \quad (\text{A8})$$

where μ is the Poisson's coefficient.

The macrostructural bulk moduli for changes in suction and temperature have been computed considering the following law:

$$K_s = \frac{(1+e_2)(s_2 + p_{atm})}{\kappa_s}; \quad K_T = \frac{1}{(\alpha_0 + \alpha_2 \Delta T)} \quad (\text{A9})$$

where κ_s is the macrostructural elastic stiffness parameter for changes in suction, α_0 and α_2 are parameters related to the elastic thermal strain.

More details related to the model formulation and its implementation in the CODE_BRIGHT program can be found in^{[6],[15]}.